Meas. Sci. Technol. 4 (1993) 249–257. Printed in the UK

Intercomparison of the effective areas of a pneumatic piston gauge determined by different techniques

K Jain†, C Ehrlich‡, J Houck‡, and J K N Sharma†

†Pressure and Vacuum Division, National Physical Laboratory, New Dehli 110012, India
‡Thermophysics Division, National Institute of Standards and Technology, Gaithersburg, MD 20899, USA

Received 15 January 1992, in final form 22 October 1992, accepted for publication 6 November 1992

Abstract. A variety of primary measurement techniques is now available for the measurement of pressure to 1 MPa and above. To ascertain the systematic uncertainty, if any, which exists in the measured pressure using the individual techniques, it is best to perform direct intercomparisons of primary instruments. However, when direct intercomparison is not possible, the next best alternative is to use a highly stable, reproducible transfer artifact such as a simple piston gauge. Such intercomparisons are described here, utilizing a piston gauge calibrated by a mercury manometer (with 0.1 MPa full-scale pressure), four large diameter 'dimensional' piston gauges from two different manufacturers (all with 1 MPa full-scale pressure), and a controlled clearance piston gauge (with 7 MPa full-scale pressure). The area ratio derived from dimensional measurements on two of the large diameter gauges, when compared with the ratio obtained from measurements traceable to a manometer, agrees within 1 part per million (ppm). For one of the large diameter piston gauges, the area value obtained from the manometer agrees within 3 ppm with its dimensional area, and within 10 ppm with the value obtained by its direct calibration against the controlled clearance piston gauge.

1. Introduction

The accurate measurement of pneumatic pressure close to the atmospheric region has become very important in meeting the increasing worldwide demands of industry and research. The primary measurement of hydrostatic pneumatic pressure at, or near, atmospheric pressure has traditionally been performed by most National Metrological Laboratories through the use of liquid column manometers [1–4], which are generally regarded as first-principles instruments. However, the operating range of these instruments has been generally limited to pressures below 0.5 MPa, their optimum performance is subject to stringently controlled conditions during operation, and they are not easily portable. Thus the use of simple piston gauges, which are portable, easier to operate, and capable of measuring higher pressures, is becoming important for transferring the unit of pressure from the manometer with only minimal loss in accuracy [5–7]. As an alternative to the manometer, primary controlled clearance piston gauges can also be used to calibrate simple piston gauges to a few MPa, although with approximately twice the uncertainty [8]. With proper precautions concerning certain observed gas species and operational mode effects [9], it is possible to use piston gauges as primary instruments, with acceptable uncertainties, by using geometrical measurements. A detailed study has been carried out to compare four simple piston gauges, denoted NIST 4, NIST 5, NIST 8 and NIST 9. These large-diameter (35 mm diameter) piston-cylinder assemblies of nominal area 1×10^{-3} m^2, and full-scale pressure of 1 MPa, have been characterized to investigate the consistency in their effective areas obtained by one or more of the following methods: (1) calibration against a standard [7, 9], which has traceability to the NIST Gas Thermometer Manometer (GTM) [1], (2) intercomparison between the assemblies, (3) dimensional metrology, or (4) calibration against a controlled clearance piston gauge [10], as represented in figure 1. The results of this study show an agreement within 10 ppm between the three independent techniques, which are based on different principles. This agreement is below the estimated total uncertainty of each technique (22 ppm for traceability to the GTM, 39 ppm for dimensional uncertainty, and 78 ppm for the controlled clearance piston gauge).

In piston gauges, a cylindrical piston rotates in a closely-fitted circular cylinder. The pressure at the base of the piston is defined as the ratio of the total downward force on the piston to the effective area of the gauge

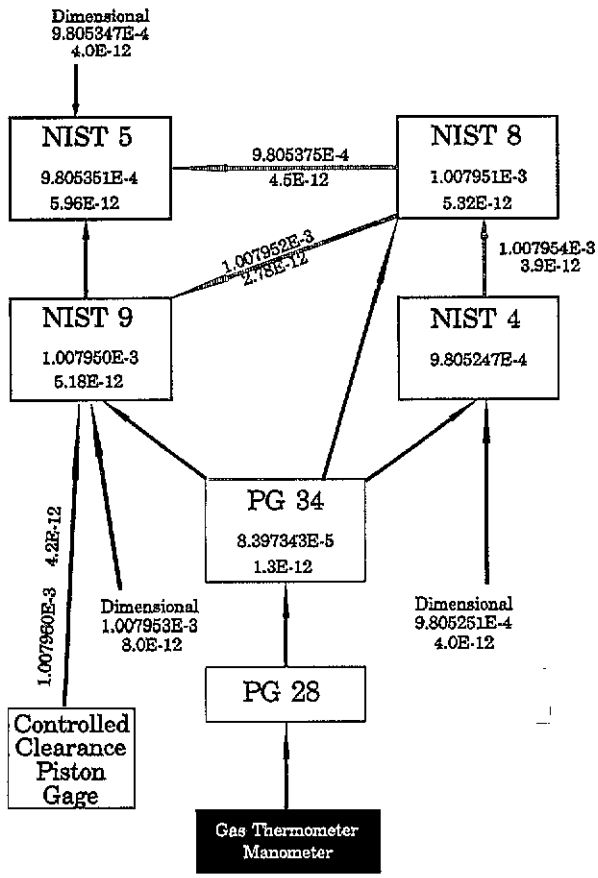

Figure 1. Schematic representation of the direct comparisons and intercomparisons of the different piston gauges. The boxes NIST 4, NIST 5, NIST 8, and NIST 9 represent the four large-diameter (35 mm) gauges, and the values in the boxes are the zero-pressure effective areas (A_0) and distortion coefficients (b) from selected comparisons (see table 2).

when floating at its operating level. The accuracy with which a pressure measurement can be made using these gauges depends on the accuracy with which measurements of both force and pressure-dependent effective area can be made. The pressure dependence of the effective area is most often due to the distortion of the piston and cylinder, and can be calculated analytically for simple geometries from the dimensions and the mechanical properties of the piston and cylinder. For a given model and at low (atmospheric) pressure [11, 12], the effective area of the piston gauge can be calculated to a level of estimated accuracy as low as several parts per million, and is essentially limited by the accuracy with which absolute dimensional measurements can be made on the piston and cylinder. At higher pressures, the estimated accuracy of the pressure measured by a gauge is limited, in addition, by how precisely the pressure distortion coefficient can be determined [13].

Constructing simple piston gauges with large diameters allows relatively improved measurement capability of cylindricity and straightness of the piston and cylinder, which gives a better determination of the low-pressure effective area. Additionally, for a given absolute uncertainty in dimensional measurement, the uncertainty in the measured area of a large-diameter piston and cylinder is reduced below that of a smaller-diameter gauge.

2. Theory

The pressure (P) generated by a pneumatic piston gauge floating at its reference level is given by [14]

$$P=\frac{\sum_{i=1}^{n}\left[M_i\left(1-\frac{\rho_{air}}{\rho_{m_i}}\right)\right]g}{A_0(1+bP)\,[1+(\alpha_p+\alpha_c)\,(T-T_r)]} \tag{1}$$

where

M_i is the true mass of the ith weight,
ρ_{air} is the density of air in the vicinity of the weights,
ρ_{m_i} is the density of the ith weight,
g is the local acceleration due to gravity,
A_0 is the effective area at the reference temperature and atmospheric pressure,
b is the pressure distortion coefficient of the piston and cylinder combination,
α_p is the linear thermal expansion coefficient of the piston,
α_c is the linear thermal expansion coefficient of the cylinder,
T is the absolute temperature of the piston and cylinder,
T_r is the absolute reference temperature.

The pressure (P_c) generated by a pneumatic controlled clearance piston gauge is given by [10]:

$$P_c=\frac{\sum_{i=1}^{n}\left[M_i\left(1-\frac{\rho_{air}}{\rho_{m_i}}\right)\right]g}{\pi\, r_p^2\,(1+b_pP)\,[1+(\alpha_p+\alpha_c)\,(T-T_r)]\,[1+d(P_z-P_j)]} \tag{2}$$

where b_p is the pressure distortion coefficient of the piston, r_p is the radius of the piston at the reference temperature and atmospheric pressure, d is the jacket pressure coefficient, P_z is the 'zero-clearance' jacket pressure, and P_j is the operating jacket pressure.

The effective area $A_{c(T)}$ of a piston gauge under test can be expressed as

$$A_{c(T)}=\{A_0\,(1+bP)\,[1+(\alpha_p+\alpha_c)\,(T-T_r)]\}_T = \frac{\sum_{i=1}^{n}\left[M_i\left(1-\frac{\rho_{air}}{\rho_{m_i}}\right)g\right]_T}{(P_s+\Delta P)} \tag{3}$$

where P_s is the pressure at the reference level of the standard gauge and ΔP is the head correction $(\rho_f-\rho_{air})gH$, where H is the height difference between the reference levels of the two gauges and ρ_f is the density of the pressure transmitting fluid. ΔP can be positive or negative depending on whether the reference level of the standard is lower or higher than that of the test gauge.

Here, these fundamental piston gauge equations have been used to evaluate the data, which are discussed below.

3. Experiment

The confidence level in all of the stated uncertainties are at the three sigma (99%) level, unless otherwise stated. Total random uncertainties are obtained as the root-sum-square of individual components, and final total uncertainties are obtained as the linear sum of the total random uncertainty and the individual systematic components, again unless otherwise stated.

3.1. Description of standards

NIST pressure standards PG28 and PG34 are commercially manufactured piston gauges with a tungsten carbide piston-cylinder assembly of simple design, and full-scale pressures of 0.3 MPa and 1.4 MPa respectively. The area of PG28 [7] was determined by direct comparison against the GTM [1], which has an uncertainty value of 2 ppm (root-sum-squared) in pressure over its full-scale value of 100 kPa. The total uncertainty (three sigma, or 3σ) associated with the effective area of PG28 is 14 ppm (linear sum) in its absolute mode of operation [7]. In the gauge mode an additional uncertainty of 5 ppm was added, based upon the differences observed between the absolute-mode and the gauge-mode effective areas of several piston gauges when directly compared against a liquid column manometer [6]. The gauge-mode effective area of PG34 was derived by its direct comparison against PG28 with an estimated uncertainty of ± 22 ppm.

3.2. National Physical Laboratory (NPL, India) controlled clearance primary pressure standard

The NPL (India) primary standard is a commercially manufactured controlled clearance piston gauge, with a full-scale pressure of 7 MPa. The piston is made of Carbaloy and the cylinder is made of non-magnetic stainless steel (SS-17-4 PH). The nominal area of the piston is 1×10^{-4} m^2. Its careful characterization gives the total uncertainty in the measured pressure of 78 ppm (three sigma) up to a pressure of 4 MPa. This is well reflected in the bilateral international intercomparison between the NPL (India) and the Physikalisch Technische Bundesanstalt (PTB, Germany) in the pneumatic pressure region, up to 4 MPa. In this comparison the low-pressure effective area of the NPL transfer standard, obtained from the NPL primary standard, agreed within 1 ppm with the value derived from the measurements using the PTB-4 standard [15].

3.3. Description of the test piston gauges

The test piston gauges are simple piston-cylinder assemblies. NIST 4 and NIST 5 have nominal low-pressure (atmospheric) areas of 9.8×10^{-4} m^2, and NIST 8 and NIST 9 have nominal low-pressure areas of 1.0×10^{-3} m^2. The gauges were procured in pairs from two different manufacturers, and all have a full-scale nominal pressure of 1 MPa. The nominal clearance between the piston and cylinder of NIST 4 and NIST 5 is 0.5 μm, and of NIST 8 and NIST 9 is 1.0 μm. The force is applied to the pistons by ring weights stacked on a weight hanger which is in direct contact with the top of the piston in the cases of NIST 4 and NIST 5, and through a ball (a part of the piston) and weight table in the cases of NIST 8 and NIST 9.

3.4. Measurement procedure for the determination of the effective area

The effective areas of the test piston gauges were sometimes determined by direct calibration or comparison by using the well-known cross-float technique [10]. A schematic experimental arrangement for the cross-float of the piston gauges is shown in figure 2. It comprises a manually operated needle valve (A) to control the gas flow to generate the desired pressure, and a ball valve (B) to isolate the piston gauges from one another. All connecting pressure lines are covered with rubber insulation to minimize temperature effects and thereby improve cross-float sensitivity. As it was not possible to bring the piston gauges to the same operating level during the cross-float, a pressure head correction term was applied in the subsequent data analysis. In all cases under consideration the reference level ranged between 1.3×10^{-2} to 2.6×10^{-1} m. As all measurements of reference level were made to an accuracy of $\pm 5.0 \times 10^{-4}$ m, representing 0.05 ppm uncertainty in pressure, this contribution to the total estimated uncertainty in the measured pressure is negligible here.

All piston gauges used were supported by a sturdy wooden base to minimize vibration and magnetic effects. All measurements were taken in an environment that provides a stable temperature of 296 ± 1 K. The temperatures of all the piston gauges were measured with

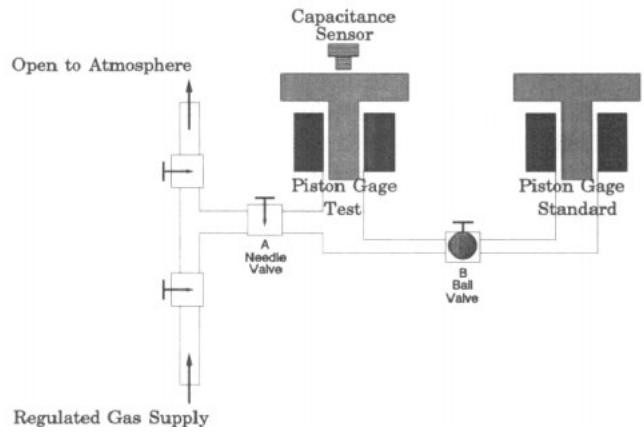

Figure 2. Experimental cross-float arrangement between the test gauge and standard piston gauge.

thermistors attached to the pressure column; the thermistors had a digital display having a resolution of 0.01 K. During the comparison of the test gauge against the controlled clearance piston gauge the temperatures of both gauges were measured using 100 Ω platinum resistance thermometers, and their outputs were read with an autoranging digital multimeter having a resolution of 1 mΩ. High purity nitrogen (99.99%) was used as the pressure transmitting fluid, irrespective of the standard, to evaluate the effective area of the test gauge. Before installation in the column, all piston-cylinder assemblies were checked for magnetic fields with a Hall probe and were demagnetized if necessary to keep the magnetic field under a few $\times 10^{-4}$ T.

Before the cross-float, both piston gauges were levelled to ensure the verticality of the axis, and the system was checked for leaks to the full-scale pressure value of 1 MPa. The piston gauges were loaded with the weights, calculated to generate the desired pressure, and then pressurized to float at their reference levels. They were then isolated from the rest of the pressurizing system by closing valve A, and subsequently from each other by closing valve B. The fall rate of the test gauge, the area of which was being evaluated, was measured using a capacitance type, linear voltage displacement transducer. The transducer output, which was directly recorded on an $X-t$ chart recorder, monitored both the position and fall rate of the piston. By adjusting the fractional weights on the test gauge, which was generating lower pressure, cross-float equilibrium was achieved, as determined when the test gauge had the same fall rate irrespective of whether valve B was closed or open. The pressure was then increased, and the same procedure was repeated, up to the full scale of 1 MPa. A period of about 30 minutes between two successive observations was found adequate to allow the system to return to equilibrium, and about 10 minutes was required to repeat observations at each pressure point.

The calibration of the test gauges against pressure standards and comparisons of the test gauges among themselves were done according to the plan shown in figure 1. NIST 4 was calibrated against PG34 and subsequently used as a cross-float standard in comparison with NIST 8. NIST 8 was then directly calibrated against PG34. In a similar way, PG34 was used to calibrate NIST 9, which was then compared, as a test gauge, with NIST 8. Finally, NIST 5 as a test gauge was compared independently with NIST 9 and then with NIST 8. NIST 9 was also calibrated by the controlled clearance piston gauge, and the effective areas of NIST 4, NIST 5 and NIST 9 were calculated from the geometrical measurements, using values of b obtained from elastic theory.

A similar procedure was used to evaluate the effective area of NIST 9 when it was cross-floated against the NPL controlled clearance piston gauge, except that an operating jacket pressure was also applied to the standard. The loads on the gauges were manually rotated clockwise so as to maintain the piston rotational speed of 25 ± 10 RPM. The speed was checked from time to time by a photoelectric switch and a counter. The controlled clearance piston gauge was rotated by a synchronous motor at about 40 RPM, and the rotations were measured with an infrared rotational detector and electronic counter having a resolution of 0.1 RPM.

At least three test cycles were carried out in all of the calibrations of any gauge. In one cycle the pressure was increased to 100, 200, 450, 600, 700, 800 and 900 kPa, and then decreased to 800, 700, 550, 360, 200 and 100 kPa. In the other two cycles, the measurement proceeded from the highest pressure to the lowest, and back to the highest. Thirteen observations were thus taken in each test cycle, leading to a total of at least 39 observations per calibration.

4. Results and discussion

One or more of four methods have been used to determine the effective areas of each of four simple test piston gauges. Three of the four test gauges have been characterized dimensionally for purposes of calculating their effective areas. The model of Meyers and Jessup [16] has been used to calculate the effective area, which assumes that there is no dependence of the viscous drag on the fluid viscosity, that the pistons and cylinders are nearly straight and free from taper, and that the effective area of the piston and cylinder assembly is very nearly the average of the mean cross-sectional area of the piston and cylinder. The estimated accuracy of the gauge is primarily limited by the uncertainty of the diametrical measurements and the deviations of the piston and cylinder from the perfect cylindrical shape. In practice, since the piston and cylinder never possess perfect geometry, one could follow the method developed by Dadson *et al* [11, 17] to derive the effective area of the gauge. In these studies, however, the value of the effective area was calculated by simply averaging the dimensional measurements taken at different points in a plane perpendicular to the piston–cylinder axis, and in different planes along the axis. The measurement process consisted of separate measurements of roundness, diameter and straightness of the piston and the cylinder. The roundness measurements were made for both items on a roundness machine at a 20 000 × magnification which produced deviations from a nominally round trace. The traces were typically made at the midpoint of each item and approximately 20 and 2.5 mm from both ends for a total of five traces. The pistons and cylinders are approximately 70 mm long. The diameter measurements were also made at approximately the same five locations along the length of each item. The diameters of both the piston and the cylinder were measured on a comparator and compared with NIST master gauge blocks of known value. For both items, the measurements were repeated after the piece had been rotated 90 degrees. The straightness measurements for both items were made along the entire length of each at four positions along the circumference, and were repeated at least twice. The ten diameter measurements of the piston were averaged to

determine the average diameter of the piston, and similarly for the cylinder. These values were then used as discussed above to calculate the effective area of the piston–cylinder combination. The roundness and straightness measurements were used primarily in aiding the assessment of the overall uncertainty of the area determination. The results of these calculations and the total estimated uncertainties associated with the area values calculated for the piston gauges NIST 4, NIST 5 and NIST 9 are listed in table 1.

A second method used to determine the effective areas of three of the test gauges, the calibration of the test gauge against a standard, was performed using the conventional cross-float technique. A computer program developed and used at NIST [18] that determines the effective area and the pressure coefficients of the test gauge based upon those of the 'standard', was used to evaluate the data. This program is based upon equations (1)–(3) above, and also provides the standard deviation of the residuals of the area, and the standard deviation of the coefficients.

NIST 4 was calibrated against PG34 at nine different pressures with a total of 39 observations in three different test cycles at each pressure. The deviations of the effective area, in ppm, for the individual measured pressures, from the best fit equation $A_e = A_o$, is shown in figure 3. Though there is slight structure in the effective area as a function of pressure, the linear fit equation of the type $A_e = A_o(1 + bP)$ differs by less than 0.5 ppm from $A_e = A_o$ over the entire pressure range. Moreover, the three-sigma standard deviation of the derived 'b' coefficient is far greater than the value of the 'b' coefficient itself, and hence the linear equation was not used. The value of $A_e = 9.805\,247 \times 10^{-4}\ m^2$ of NIST 4 obtained from the calibration by PG34 agrees, to within 0.5 ppm, with the value of $9.805\,251 \times 10^{-4}\ m^2$ calculated from the geometry of the piston and cylinder assembly for low pressures. The theoretical value of the distortion coefficient $b = 4.0 \times 10^{-12}\ Pa^{-1}$, calculated from elastic theory [12] using an elastic modulus of the cylinder material $(E_c) = 6.3 \times 10^{11}$ Pa and Poisson's ratio of $\mu_c = 0.218$, was also used in the calculation of A_e. At the full-scale pressure value of 1 MPa the difference from the experimental value increases to 4 ppm. The values of A_e lie well within the level of total estimated uncertainties of PG34 and the geometrical measurements.

The experimental value of A_e of NIST 4, obtained by its calibration against PG34, was also used in the comparison of NIST 8 with NIST 4. During this comparison, four pressure cycles were carried out, for a total of 56 observations. The linear best fit equation is $A_e = 1.007\,954 \times 10^{-3}\ (1 + 3.9 \times 10^{-12} P)$ where A_e is an m^2 and P is in Pa. The deviation of the effective area at each measured pressure was within 2.5 ppm over the entire range of pressure, and the residuals showed no pressure-dependent structure. The value of the low-pressure area (A_o) and the pressure coefficient b, and associated three-sigma uncertainties, are given in table 2. The linear best fit equation $A_e = 1.007\,951 \times 10^{-3}\ (1 + 5.32 \times 10^{-12} P)$ was also obtained by calibrating NIST 8 against PG34 at the nine discrete pressures. Three test cycles were carried out leading to a total of 42 observations. The values of A_o and b, and their three-sigma standard deviations, are also given in table 2.

To visualize the degree of closure of the effective area between the two independent comparisons associated with NIST 8, the effective areas calculated from the linear best fit equations mentioned above, as a function of nominal pressure, are shown in figure 4. This figure shows that systematic differences of 3 ppm at 100 kPa and 2 ppm at 900 kPa exist between the two independent comparisons. This is mainly due to the difference of 3 ppm in the low pressure effective area values obtained in the two independent comparisons, as the difference in

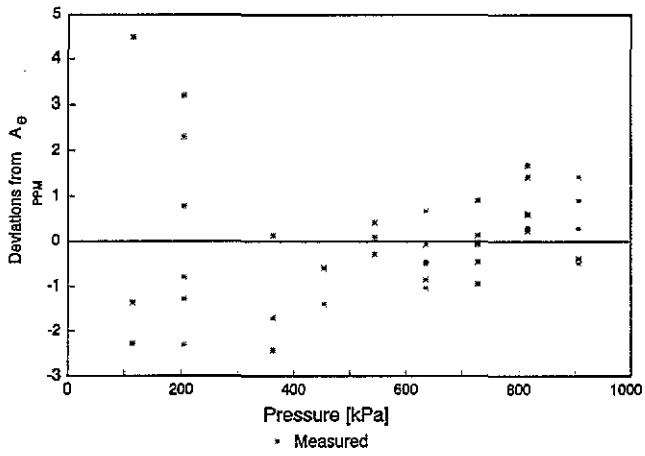

Figure 3. Deviations of measured values of the effective area (A_e) of NIST 4 from the best fit ($A_e = 9.805\,247 \times 10^{-4}\ m^2$), when calibrated by PG34.

Table 1. Area of piston gauges as calculated by geometrical measurements.

Piston gauge designation	NIST4	NIST5	NIST9
Effective area at atmospheric pressure and at 23°C (m^2)	$9.805\,251 \times 10^{-4}$	$9.805\,347 \times 10^{-4}$	$1.007\,953 \times 10^{-4}$
Elastic distortion calculated from simple elastic theory (Pa^{-1})	4.0×10^{-12}	4.0×10^{-12}	8.0×10^{-12}
Estimated total uncertainty in the area $\Delta A_o/A_o$ (ppm) *(three sigma)*	17	19	39

Table 2. Summary of calibrations/comparisons of the test piston gauges.

Standard gauge			Test gauge					
Std	A_0(Std)	b(Std) (MPa^{-1})	Test	A_0	3σ A_0 (ppm)	b (MPa^{-1})	3σ b (MPa^{-1})	3σ A_e (ppm)
PG34	$8.397\,343\times10^{-5}$	1.3×10^{-6}	NIST4	$9.805\,247\times10^{-4}$	0.6	—	—	4
PG34	$8.397\,343\times10^{-5}$	1.3×10^{-6}	NIST8	$1.007\,951\times10^{-3}$	1	5.32×10^{-6}	1.7×10^{-6}	2.8
PG34	$8.397\,343\times10^{-5}$	1.3×10^{-6}	NIST9	$1.007\,950\times10^{-3}$	0.7	5.18×10^{-6}	1.2×10^{-6}	2
NIST4	$9.805\,247\times10^{-4}$	—	NIST8	$1.007\,954\times10^{-3}$	0.7	3.9×10^{-6}	1.2×10^{-6}	2.5
NIST8	$1.007\,951\times10^{-3}$	5.32×10^{-12}	NIST9	$1.007\,952\times10^{-3}$	0.7	2.78×10^{-6}	1.2×10^{-6}	2
NIST9	$1.007\,950\times10^{-3}$	5.18×10^{-12}	NIST5	$9.805\,351\times10^{-4}$	0.7	5.96×10^{-6}	1.1×10^{-6}	2
NIST8	$1.007\,951\times10^{-3}$	5.32×10^{-12}	NIST5	$9.805\,375\times10^{-4}$	0.6	4.5×10^{-6}	1.0×10^{-6}	2
NPLCC-1	$1.000\,692\times10^{-4}$	(Nominal)	NIST9	$1.007\,960\times10^{-3}$		4.2×10^{-6}		

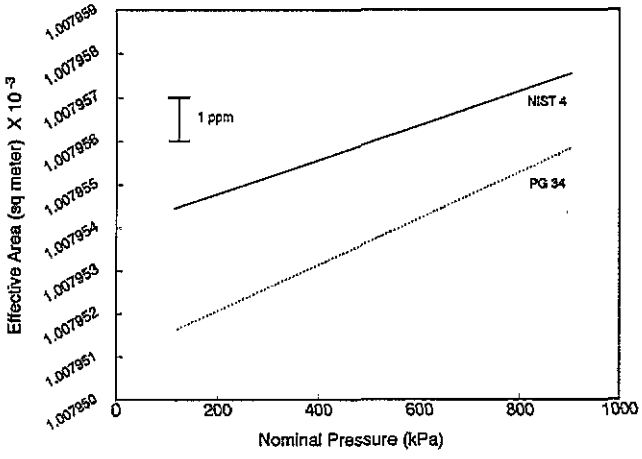

Figure 4. Effective area of NIST 8 as obtained by its direct calibration against PG34 and NIST 4.

the b values obtained in these comparisons would not cause deviation in the A_e values of more than 1 ppm over the entire range of pressure. Though the differences in the A_0 values are outside of their three-sigma standard deviations (table 2), the A_0 values agree well, considering the total estimated uncertainties of PG34 and NIST 4 individually (table 3).

The PG34 pressure standard was also used to calibrate NIST 9 at nine different pressures with a total of 42 observations in three different test cycles. The deviations of the effective area, in ppm, for the individual measured pressures, from the best fit linear equation $A_e = 1.007\,950\times10^{-3}\,(1+5.18\times10^{-12}P)$, where A_e is in m^2 and P is in Pa, are shown in figure 5. The effective area of NIST 9 when characterized by NIST 8 is $A_e = 1.007\,952\times10^{-3}\,(1+2.78\times10^{-12}P)$. A difference of only 2 ppm exists between the values of A_0 obtained in these two comparisons, and a difference of 3 ppm exists with the value calculated from the geometrical measurements on NIST 9. The ratio of the A_0 values of NIST 9 and NIST 4 obtained from their direct calibration by PG34 agrees within 2.6 ppm with the same ratio obtained from their geometrical characterizations. This is consistent with the above 3 ppm difference.

The A_e values of NIST 9 obtained from its direct calibration against PG34 differ by 3 ppm at 100 kPa, increasing to 6 ppm at 1 MPa, with the A_e values calculated from the geometrical area and incorporating the value of $b = 8\times10^{-12}\ Pa^{-1}$ calculated from simple elastic theory. This is mainly due to the difference in the b values obtained experimentally and calculated from elastic theory. Though the experimentally determined values of b of NIST 9 from PG34 and NIST 8 differ between themselves in their absolute values, this results in a difference of less than 2 ppm in the values of A_e over the entire range of pressure. This is well within the three-sigma standard deviations of A_e (table 2). Although the calculated A_e value differs by 6 ppm at 1 MPa from the experimental value, this is still well within the total estimated uncertainties of the individual techniques (tables 1 and 3).

Due to the relatively large differences in the values of b of NIST 9 obtained experimentally and by calculation, it is desirable to check the consistency of the effective area of NIST 9 obtained by its direct calibration against PG34 by comparing the remaining test gauge, NIST 5, with NIST 9, and also with NIST 8, using the effective area of NIST 8 obtained by its direct calibration against PG34. This will show if any relative systematic error exists in the effective areas of NIST 8 and NIST 9, and will also increase confidence in their uncertainties.

NIST 5 was compared with NIST 9 at nine different pressures for a total of 56 observations. The deviations of the effective area, in ppm, for the individual measured pressures, from the linear best fit equation $A_e = 9.805\,351\times10^{-4}\,(1+5.96\times10^{-12}P)$, where A_e is in m^2 and P is in Pa, are shown in figure 6. Similar scatter in the residuals (observed minus calculated) of the effective area of NIST 5 is also observed when NIST 5 is compared with NIST 8. The values of A_0 and b, along with their uncertainties, are given in table 2. The difference between the effective area of NIST 5 obtained by comparison with NIST 8, $A_e = 9.805\,375\times10^{-4}\,(1+4.5\times10^{-12}P)$, and the effective area of NIST 5 obtained experimentally by its direct comparison with NIST 9, is also shown in figure 6, by the dotted line. The effective area agrees within 2.5 ppm over the entire

Table 3. *Metrological characteristics (known and measured) of the piston gauges.*

Piston gauge	NIST4	NIST5	NIST8	NIST9
Piston–cylinder (Type)	Simple	Simple	Simple	Simple
Full scale pressure (MPa)	1	1	1	1
Piston material	Tungsten carbide	Tungsten carbide	Tungsten carbide	Tungsten carbide
Cylinder material	Tungsten carbide	Tungsten carbide	Tungsten carbide	Tungsten carbide
Fluid	Nitrogen	Nitrogen	Nitrogen	Nitrogen
Coefficient of thermal expansion for piston ($°C^{-1}$)	4.5×10^{-6}	4.5×10^{-6}	4.11×10^{-6}	4.11×10^{-6}
Coefficient of thermal expansion for cylinder ($°C^{-1}$)	4.5×10^{-6}	4.5×10^{-6}	4.11×10^{-6}	4.11×10^{-6}
Effective area at atmospheric pressure and at 23°C (m^2)	$9.805\,247 \times 10^{-4}$	$9.805\,351 \times 10^{-4}$	$1.007\,951 \times 10^{-3}$	$1.007\,950 \times 10^{-3}$
Distortion coefficient (Pa^{-1})	—	5.96×10^{-12}	5.32×10^{-12}	5.18×10^{-12}
Estimated total uncertainty of the effective area $\Delta A_e/A_e$ (ppm)	26	26	26	24

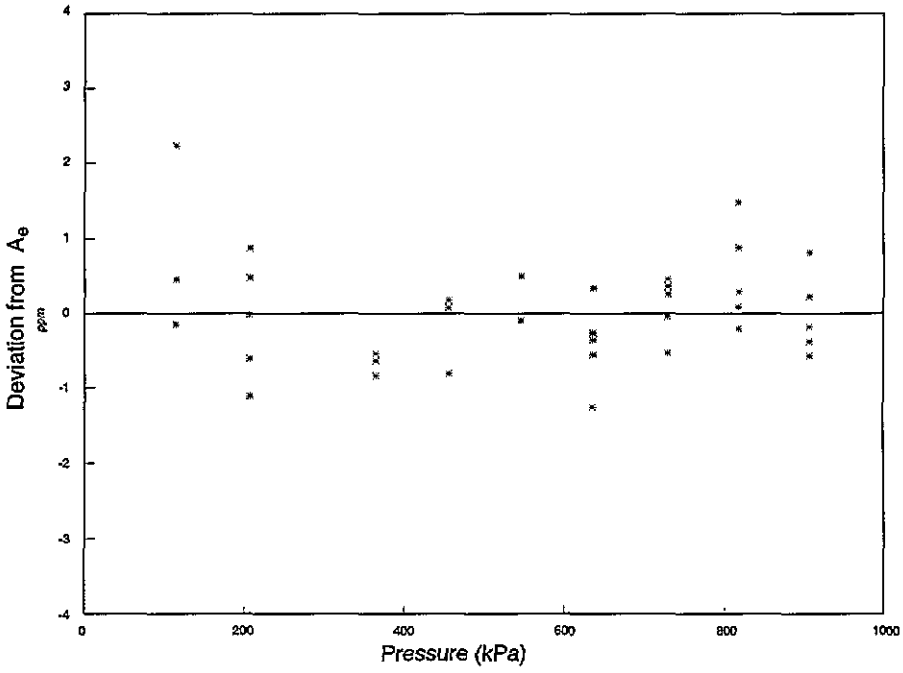

Figure 5. Deviations of measured values of the effective area (A_e) of NIST 9 from the linear best fit ($A_e = 1.007\,95 \times 10^{-3}(1 + 5.18 \times 10^{-12}P)$ where A_e is in m^2 and P is in Pa), when calibrated by PG34.

range of pressure, as expected. This is consistent with the individual three sigma standard deviations of the A_e values of 2 ppm. Further, the ratio of the experimentally determined values of A_0 of NIST 9 and NIST 5 agree within 3 ppm with the ratio of the A_0 values calculated geometrically. Agreement of 1.5 ppm at 1 MPa is obtained, as expected, between the values of b of NIST 5 by comparison with NIST 9 and NIST 8, providing confidence in the respective effective areas assigned to the two gauges.

To investigate further the consistency between the determinations of the effective areas of NIST 9, a direct comparison can be made of the low pressure area (A_0) ratios of NIST 9 and NIST 8, obtained in different ways, such as:

$$(\text{NIST9/NIST5})_{A_0} = 1.027\,9591$$

$$(\text{NIST8/NIST5})_{A_0} = 1.027\,9576,$$

from which we obtain:

$$(\text{NIST9/NIST8})_{A_0} = 1.000\,0015.$$

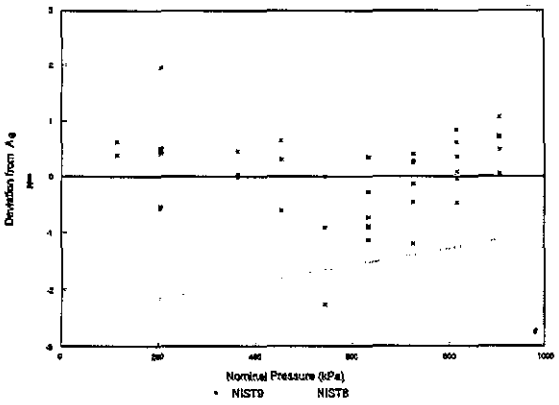

Figure 6. Points show the deviations of measured values of the effective area (A_e) of NIST 5 from the best linear fit ($A_e = 9.805\,351 \times 10^{-4}\,(1 + 5.96 \times 10^{-12}P)$ where A_e is in m^2 and P is in Pa), when compared with NIST 9. The dotted line represents the calculated effective area using $A_e = 9.805\,375 \times 10^{-4}\,(1 + 4.5 \times 10^{-12}P)$, obtained by the direct comparison of NIST 5 with NIST 8.

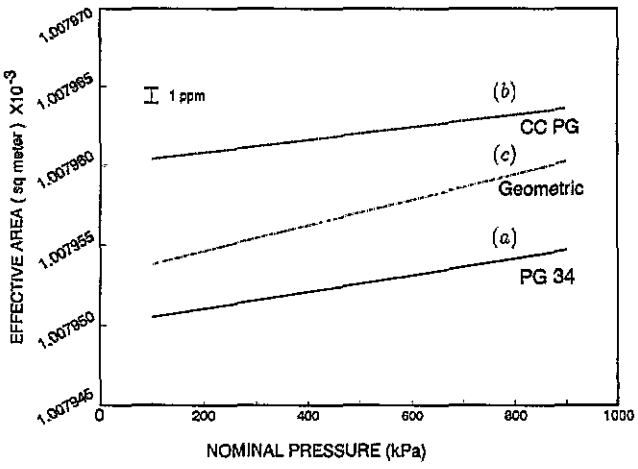

Figure 7. The effective areas of NIST 9 are plotted as a function of nominal pressure. Curves (*a*), (*b*) and (*c*) represent the effective areas of NIST 9 when calibrated by PG34, when compared with a controlled clearance gauge, and when calculated from geometrical measurements and simple elastic theory respectively.

Direct comparison of NIST9 with NIST8 gives:

$$(\text{NIST9/NIST8})_{A_0} = 1.000\,0010.$$

Using the A_0 values of NIST 9 and NIST 8 obtained directly from their calibration by PG34 gives the ratio:

$$(\text{NIST9/NIST8})_{A_0} = 0.999\,9990.$$

These last three area ratios agree to within 2.5 ppm, providing further confidence in the respective effective areas assigned to the two gauges. To the precision of the observations made, the total estimated uncertainty in the effective areas of NIST 8 and NIST 9 is ± 25 ppm over the entire pressure range, of which 2–3 ppm is regarded as the random contribution.

To further determine the level of agreement of the effective areas of NIST 9 obtained by the different primary methods, NIST 9 was also calibrated by a controlled clearance piston gauge, yielding $A_e = 1.007\,960 \times 10^{-3}\,(1 + 4.2 \times 10^{-12}P)$, where A_e is in m^2 and P is in Pa. When NIST 9 is calibrated by PG34, the effective area of NIST 9 is $A_e = 1.007\,950 \times 10^{-3} \times (1 + 5.18 \times 10^{-12}P)$. When the effective area of NIST 9 is calculated using A_0 from the detailed geometrical measurements and b from simple elastic theory, $A_e = 1.007\,953 \times 10^{-3}(1 + 8.0 \times 10^{-12}P)$. These values of the effective area of NIST 9 are plotted as a function of the pressure in figure 7. The values of the pressure-dependent effective areas A_e of NIST 9 differ between themselves, over the entire pressure range, within 10 ppm, which is well outside the individual three-sigma standard deviations as observed during its calibration by PG34 or the controlled clearance piston gauge. However, this difference is well below the estimated total uncertainty of the individual standards and also below the uncertainty in the geometrical measurements. These measurements of A_e for NIST 9 are thus all consistent within 10 ppm.

From all of the calibrations of NIST 4, NIST 8 and NIST 9 against PG34, and the intercomparisons of these test gauges, and the dimensional characterizations of NIST 4 and NIST 9, it may be concluded that the effective areas of these test gauges have an estimated total uncertainty between ± 24 and ± 26 ppm over the full-scale pressure of 1 MPa (table 3). These uncertainties represent the combined systematic uncertainty of PG34 (± 22 ppm) with the random uncertainties of the individual calibrations against PG34, given in the last column of table 2. The estimated total uncertainty of NIST 5 is then ± 26 ppm, as obtained when it was compared with NIST 9. Thus, from all of these comparisons and calibrations, it may be concluded that the effective areas of all the test gauges have an estimated total uncertainty no greater than ± 26 ppm over the full-scale pressure of 1 MPa, with the exception of NIST 9, on which dimensional measurements were performed in a laboratory having larger uncertainties (± 39 ppm) (table 1) than the laboratory in which NIST 4 and NIST 5 were measured.

5. Conclusions

The uncertainty in the effective areas of all of the test gauges could be further improved either by reducing the uncertainty in the effective area of PG34 or by making the geometrical measurements with better accuracy. Before increased confidence can be placed in the effective area values derived by the geometrical measurements, it is important to understand better the effects of factors such as the molecule–surface interaction, the pressure profile and the flow of the gas through the crevice between the piston and the cylinder. Once a good understanding of these effects is obtained, it may be possible that larger-diameter piston gauges with simple geometry could be characterized on the basis of geometrical measurements and used as primary standards

with a higher degree of confidence. It is encouraging to see, however, that the overall level of agreement between the three different techniques used to characterize NIST 9 is well within the estimated total uncertainties of the individual techniques.

References

[1] Guildner L A, Stimson H F, Edsinger R E and Anderson R L 1970 *Metrologia* **6** 1

[2] Riety P and Lecollinet P 1977 *Bull. BNM* **28** 13

[3] Jager J, Klingenberg G and Schultz W 1990 *PTB-Mitteilungen* **100** 429
Klingenberg G and Ludicke F 1991 *PTB-Mitteilungen* **101** 7

[4] Heydemann, P L M, Tilford C R and Hyland R W 1977 *J. Vac. Sci. Technol.* **14** 597

[5] Stuart P R 1989 *High Pressure Metrology* (*Monographie* 89/1) ed G F Molinar (Sèvres: Bureau International des Poids et Mesures) p 95

[6] Tilford C R, Hyland R W and Yi-tang Sheng 1989 *High Pressure Metrology*, (*Monographie* 89/1) ed G F Molinar (Sèvres: Bureau International des Poids et Mesures) p 105

[7] Welch B E, Edsinger R E, Bean V E and Ehrlich C D 1989 *J Res. Nat. Inst. Stand. and Tech.* **94** 343

[8] Sharma J K N, Jain K K and Bandyopadhyay A K 1988 *Rev. Sci. Instrum.* **59** 2063

[9] Welch B E, Edsinger R E, Bean V E and Ehrlich C D 1989 *High Pressure Metrology* (*Monographie* 89/1) ed G F Molinar (Sèvres: Bureau International des Poids et Mesures) p 81

[10] Sharma J K N, Jain K K and Badyopadhyay A K 1988 *Japan. J. Appl. Phys.* **27** 843

[11] Dadson R S, Lewis S L and Peggs G N 1982 *The Pressure Balance: Theory and Practice* (National Physical Laboratory, Teddington, England: HMSO)

[12] Heydemann P L M and Welch B E 1975 *Experimental Thermodynamics* vol II, ed B LeNeindre and B Vodar (Guildford: Butterworth) p 147

[13] Bean V E 1986 *Physica* B **139&140** 739

[14] Sharma J K N, Jain K K and Kamlesh K 1986 *Pramana* **27** 417

[15] Sharma J K N Jain K K, Badyopadhyay A K and Jager J 1988 *J. Phys. E: Sci. Instrum.* **21** 635

[16] Meyers C H and Jessup R S 1931 *J. Res. NBS* **6** 1061

[17] Dadson R S, Greig R G P and Horner A 1965 *Metrologia* **1** 55

[18] Houck J C, Molinar G F and Maghenzani R 1983 *J. Res. NBS* **88** 253